

## SdiA Degeneracy in *Klebsiella pneumoniae*: Insights from Molecular Docking Studies

Janki Panchal<sup>1</sup>, Milan Dabhi<sup>1</sup>, Arun Patel<sup>2</sup>, Sandip Patel<sup>2</sup>, Dweipayan Goswami<sup>1\*</sup>

<sup>1</sup>Department of Microbiology & Biotechnology, University School of Sciences, Gujarat University, Ahmedabad 380009, Gujarat, India.

<sup>2</sup>Department of Veterinary Microbiology, College of Veterinary Sciences & Animal Husbandry, Sardarkrushinagar 385505, Kamdhenu University, Gujarat, India.

Janki Panchal (ORCID:0009-0007-8235-568X)

Milan Dabhi (ORCID: 0000-0001-6581-8389)

Arun Patel (ORCID: 0000-0002-1525-3663)

Sandip Patel (ORCID: 0000-0001-9235-9413)

Dweipayan Goswami (ORCID: 0000-0003-0165-0294)

Email: [dweipayan.goswami@gujaratuniversity.ac.in](mailto:dweipayan.goswami@gujaratuniversity.ac.in)

### ABSTRACT

*SdiA* is a regulatory protein that plays a crucial role in controlling the expression of virulence factors in *Klebsiella pneumoniae*, which helps the bacterium to evade the host immune system and adhere to host tissues. Unlike most Gram-negative bacteria, *K. pneumoniae* does not produce its own AHLs but instead responds to exogenous AHLs produced by other bacterial species through its orphan LuxR-type receptor, SdiA. Due to the promiscuity in ligand binding, SdiA exhibits a degenerate nature as it can bind to various AHLs and AI-2. In this study, the specific interactions and ligand preferences of SdiA were investigated to determine the degree of degeneracy of this protein. As the crystallized structure of SdiA of *K. pneumoniae* is not available, its 3D model was predicted using homology modeling. All possible auto-inducers (AHLs and AI-2 ligands) were docked with the modelled SdiA using molecular docking studies to understand the probable interactions and ligand preferences. The results showed that 3-OH-C10-HSL, 3-OH-C8-HSL, 3-oxo-C10-HSL, 3-oxo-C8-HSL, 3-oxo-C12-HSL, and C10-HSL interacted best with SdiA, while AI-2s (THMF and HMF) showed poor docking scores. AHLs with shorter chains exhibited moderate affinity. The ability of SdiA to bind to multiple AHLs and potentially AI-2 confers functional advantages, allowing *K. pneumoniae* to eavesdrop on the quorum sensing signals of other bacterial species in mixed microbial communities. The findings of this study provide insights into the ligand preferences and interactions of SdiA with AHLs and AI-2 and offer a basis for developing new approaches to combat *K. pneumoniae* infections.

**Keywords:** *Klebsiella pneumoniae*; SdiA; Quorum sensing; Auto-inducers; Homology modelling; Molecular Docking

Received 11.05.2023

Revised 04.06.2023

Accepted 21.06.2023

### How to cite this article:

Janki Panchal, Milan Dabhi, Arun Patel, Sandip Patel, Dweipayan Goswami. SdiA Degeneracy in *Klebsiella pneumoniae*: Insights from Molecular Docking Studies. Adv. Biores. Special Issue 1: 2023: 23-35

### INTRODUCTION

*Klebsiella pneumoniae* is a ubiquitous Gram-negative bacterium belonging to the family Enterobacteriaceae, which is considered a pathogen responsible for a wide range of human infections, such as pneumonia, urinary tract infections, bloodstream infections, and wound infections. *K. pneumoniae* is classified as an opportunistic pathogen, causing disease in individuals with compromised immune systems or underlying medical conditions [1]. *K. pneumoniae* commonly colonizes the gastrointestinal tract of healthy individuals, and it has been detected in environmental samples such as soil and water [2]. It has the capability of forming biofilms, which are protective slimy layers of cells that adhere to surfaces, providing resistance to environmental stressors and antibiotics, rendering treatment challenging. Multidrug-resistant (MDR) strains of *K. pneumoniae*, known as carbapenem-resistant Enterobacteriaceae (CRE), have recently become a significant public health issue [3]. These strains are resistant to multiple classes of antibiotics, posing a serious threat to the treatment of bacterial infections. Recently, large number of efforts are made to control MDR microbes by targeting the Quorum sensing pathways in bacteria. Quorum sensing is a process used by bacteria to communicate with each other and coordinate their behavior. Gram-negative bacteria rely on quorum sensing to regulate numerous functions, including virulence, biofilm formation, motility, and

antibiotic resistance [4]. Autoinducers are small signaling molecules specific to each bacterial species, synthesized by enzymes encoded by quorum sensing genes within the bacteria [5]. The most common autoinducer produced by Gram-negative bacteria is N-acyl-homoserine lactone (AHL), synthesized by LuxI-type proteins [6], which diffuse freely across the cell membrane and accumulate in the environment as cell density increases [7]. Once the AHL concentration reaches a certain threshold, it binds to its cognate receptor, typically a LuxR-type protein within the cell, leading to the activation or repression of specific genes [8]. Another autoinducer used by Gram-negative bacteria is autoinducer-2 (AI-2), a furanosyl borate diester molecule synthesized by the LuxS enzyme. Unlike AHLs, AI-2 is produced by a wide range of bacterial species and plays a role in interspecies communication, biofilm formation, and bacterial pathogenesis [9]. Quorum sensing in Gram-negative bacteria also influences bacterial motility and contributes to the formation of multicellular structures, such as swarms and biofilms. Moreover, it regulates gene expression involved in nutrient uptake and utilization, contributing to bacterial growth and survival [10]. Understanding quorum sensing mechanisms may lead to developing new strategies to combat bacterial infections and overcome antibiotic resistance. The regulatory protein SdiA (short for "suppressor of cell envelope damage induced by ampicillin") controls virulence factors, including capsule polysaccharides and fimbriae, allowing *K. pneumoniae* to adhere to host tissues and evade the immune system [11]. Unlike most Gram-negative bacteria, *K. pneumoniae* does not produce its own autoinducing AHLs but instead encodes an orphan LuxR-type receptor that responds to exogenous AHLs produced by other bacteria in the environment [8]. SdiA plays a crucial role in regulating virulence genes, biofilm formation, and antibiotic resistance [11]. SdiA controls operons, including *rcaA-rcaB-rcaC*, which synthesizes capsular polysaccharides, necessary for biofilm formation and evading the host immune system [12]. SdiA also activates the *kvgAS* operon, increasing virulence-associated genes and pathogenicity. By regulating outer membrane porin genes, *ompK35* and *ompK36*, SdiA modulates *K. pneumoniae*'s susceptibility to antibiotics [13]. This regulatory mechanism allows *K. pneumoniae* to adapt to environmental changes and compete with other bacterial species [14]. Understanding this mechanism is critical in developing new approaches to fight *K. pneumoniae* infections. Interestingly, SdiA can bind to multiple AHLs and potentially AI-2, demonstrating promiscuity in ligand binding can indeed be considered somewhat degenerate laid the foundation of current research described in the manuscript [12]. However, it is important to note that degeneracy is not necessarily a negative attribute for a protein, as it can offer certain functional advantages. In the case of *K. pneumoniae*, the ability of SdiA to interact with multiple AHLs and possibly AI-2 may enable the bacterium to eavesdrop on the quorum sensing signals of other bacterial species in mixed microbial communities [15]. This can be advantageous for *K. pneumoniae* as it can modulate its gene expression and behavior based on the population density and species composition of the surrounding environment [16]. In this study, we aim to understand the specific interactions and affinity of SdiA with various AHLs and AI-2. Thorough molecular docking studies are necessary to achieve this goal, even though SdiA exhibits some level of ligand binding promiscuity [12]. Understanding the behavior of SdiA with AHLs and AI-2 is crucial in developing inhibitors. As the crystallized structure of SdiA from *K. pneumoniae* is not available in the Protein Data Bank (PDB), we modeled it in this study. We then docked all possible AHLs and AI-2 ligands to investigate the probable interactions and SdiA's ligand preferences. Computational studies made this possible, and to the best of our knowledge, this is the first study to access the degeneracy of SdiA in this manner.

## MATERIAL AND METHODS

### Homology modelling of SdiA

The 3D modelling of *K. pneumoniae*'s SdiA was performed using homology modelling in SWISS-MODEL. The homology modelling method is based on the assumption that the amino acid sequence of the target protein shares significant sequence similarity with the template protein [17]. In this case, the crystal structure of SdiA of *E. coli* (PDB ID: 4Y15) was used as a template to model *K. pneumoniae*'s SdiA. The amino acid sequence of *K. pneumoniae*'s SdiA was retrieved from UniProt (ID: A0A377Y234) and used to build the model. The homology modelling approach is widely used in structural biology to predict protein structures when experimental data is not available. After modelling the protein, the quality of the modelled protein was assessed using different methods. One such method is the QMEAN analysis, which provides an estimate of the model quality based on various structural features such as the packing of atoms, the quality of backbone and side-chain geometry, and the solvent accessibility of residues. In this case, the QMEAN and QMEANDisCo analysis of the modelled protein was performed using the SWISS-MODEL server [18]. The QMEAN Z-scores provide information on the quality of individual aspects of the structure, such as the all-atom, C $\beta$ , torsion, and solvation. The QMEAN and QMEANDisCo analysis helps to evaluate the overall quality of the modelled protein. The Ramachandran plot analysis was performed using MolProbity v4.4 to

check the psi and phi angles of the modelled SdiA to check the overall torsion of the residues. The Ramachandran plot analysis provides information on the backbone torsion angles phi ( $\phi$ ) and psi ( $\psi$ ) of residues in the protein structure. The plot shows the distribution of residues in different regions of the plot, including the most favored regions, allowed regions, and disallowed regions [19]. The Ramachandran plot analysis helps to evaluate the quality of the modelled protein by checking the conformational quality of the backbone.

### **Protein and Ligand preparations**

The protein SdiA of *E. coli* was retrieved from Protein databank (PDB ID: 4Y15). The SdiA of *K. pneumoniae* was modelled using homology modelling in SWISS MODEL. The co-ordinates of SdiA was determined using UCSF Chimera [20]. Prior to docking studies, all the co-crystallized residues were removed in UCSF Chimera. The protein structure was then prepared by assigning the hydrogen atoms, charges and energy minimization using Dock Prep tool [21]. The charges were assigned as per the Gasteiger method which quickly and efficiently generates high-quality atomic charges for protein and the charges were computed using ANTECHAMBER algorithm [22]. The energy minimization was performed using 500 steepest descent steps with 0.02 Å step size and an update interval of 10. All the steps mentioned were performed in UCSF Chimera.

All the ligands used for the in-silico interaction were AI-1 and AI-2 represented from the different organisms as mentioned in the Table 1. These all ligands were retrieved from PubChem. Before performing the molecular docking of ligand and receptor, the ligands were optimized by addition of hydrogen and energy minimization using Gasteiger algorithm [23] in structure editing wizard of UCSF Chimera, which works on the chemoinformatic principle of electronegativity equilibration, and the files were saved in mol2 format. Receptor–ligand docking analysis was performed using AutoDock Vina and the program was executed as an add-on in Chimera [20].

### **Molecular docking**

Receptor-ligand docking analysis was performed using AutoDock Vina [23]. and the program was executed as an add-on in UCSF Chimera. The ligand binding of SdiA of *K. pneumoniae* was based on the crystallized ligand found in SdiA of *E. coli* (PDB ID: 4Y15) which was used as template to model SdiA of *K. pneumoniae*. In the AutoDock Vina algorithm [24], the following parameters were set as: (i) number of binding modes- 10; (ii) exhaustiveness of search- 8 and (iii) maximum energy difference- 3 kcal/mol. Out of all the possible poses suggested by Auto Dock Vina, the pose showing maximum hydrogen bonds and minimum binding free energy change (kcal/mol) as represented in the ViewDock window were chosen [25]. They were further analyzed in Biovia Discovery Studio (DS) visualizer for hydrogen bond formation, Pi sigma, alkyl/Pi alkyl, carbon hydrogen bond, etc., by the functional groups of ligands with amino acids.

## **RESULTS AND DISCUSSION**

### **Homology modelling**

The modelled SdiA structure of *K. pneumoniae* based on *E. coli* SdiA (PDB ID: 4Y15) using homology modelling in SWISS MODEL appears to be of good quality with a MolProbity score of 0.85. The Ramachandran favored percentage is 94.87%, which indicates that the majority of the residues are in favorable regions. However, there are some outliers in the Ramachandran plot, with LEU141 and PRO142 being the outliers. The rotamer outlier percentage is 0.96%, with GLU171 and ASN127 being the outliers. C-beta deviations of four residues, including LEU141, HIS128, GLU38, and ASN223, suggest that the distance between the C-beta atoms of adjacent residues is outside the expected range. The model has no bad bonds, but there are 19 bad angles, including LEU141, ASN127, (LEU141 -PRO142), HIS92, HIS128, HIS214, ASP102, HIS183, HIS15, HIS48, PHE180, HIS70, (ARG140 -LEU141). These angles are not within the expected range. The model also has two out of 14 cis-prolines, including VAL50 -PRO51 and LEU141-PRO142. The QMEANDisCo Global score of  $0.83 \pm 0.05$  indicates that the modelled SdiA structure is of good quality. However, the QMEAN score of -1.1 suggests that the overall model quality is slightly below average. The C-beta and torsion QMEAN Z-scores of -1.19 and -1.29, respectively, also indicate below-average quality. The all-atom and solvation QMEAN Z-scores of 0.76 and 0.9, respectively, indicate above-average quality in those aspects. Lastly, the modelled SdiA structure of *K. pneumoniae* using homology modelling in SWISS MODEL based on *E. coli* SdiA (PDB ID: 4Y15) appears to be of good quality. However, there are some outliers in the Ramachandran plot, rotamer outliers, bad angles, and C-beta deviations. The QMEAN score suggests that the overall model quality is slightly below average, but the all-atom and solvation QMEAN Z-scores indicate above-average quality in those aspects. Further validation and refinement of the model may be necessary to improve its accuracy and reliability. The present study investigated the degree of SdiA degeneracy in *K. pneumoniae* by studying its specific interactions and ligand preferences with various AHLs and AI-2 using molecular docking studies. The results showed that SdiA exhibits a promiscuous nature in

ligand binding and can bind to various AHLs and potentially AI-2, which confers functional advantages to *K. pneumoniae* in mixed microbial communities [26]. The top four ligands that exhibited the highest binding affinities and crucial hydrogen bond interactions with key amino acids of SdiA were identified as 3-OH-C10-HSL, 3-OH-C8-HSL, 3-oxo-C10-HSL, and 3-oxo-C8-HSL [27]. Conversely, THMF and HMF were found to be the two worst ligands in terms of binding affinity and interactions with the protein receptor. The present study utilized homology modelling to predict the 3D structure of SdiA of *K. pneumoniae*, as the crystallized structure of the protein is not available. The homology modelling approach is widely used in structural biology to predict protein structures when experimental data is not available, and it is based on the assumption that the amino acid sequence of the target protein shares significant sequence similarity with the template protein [28]. Previous studies have also utilized homology modelling and molecular docking to investigate the interaction between SdiA and AHLs in other bacterial species [28]. For instance, a study by Li and colleagues in the year 2015 used homology modelling and molecular docking to investigate the interaction between SdiA of *Salmonella enterica* and various AHLs [29]. The study identified several key amino acids that play a crucial role in ligand binding and showed that SdiA has a high degree of promiscuity in ligand binding [12]. Similarly, a study by Ma and colleagues in the year 2017 utilized homology modelling and molecular docking to investigate the interaction between SdiA of *Erwinia carotovora* and various AHLs [30]. The study identified several key amino acids that contribute to the binding affinity of the ligand to the protein receptor and showed that SdiA exhibits a high degree of degeneracy in ligand binding [26].

#### **Comparison of SdiA of *E. coli* with modelled SdiA of *K. pneumoniae***

In this study, we compared the binding interactions of the quorum sensing molecule 3-oxo-6-HSL with SdiA proteins from two different bacterial species, *Escherichia coli* and *Klebsiella pneumoniae*. The crystal structure of SdiA from *E. coli*, with (PDB ID 4Y15), was used as a template to generate a homology model of SdiA from *K. pneumoniae*. The comparison of ligand-binding interactions in these proteins was visualized in Figure 2. In the case of *E. coli* SdiA (PDB ID: 4Y15), the protein forms hydrogen bonds with TRP67, SER43, and SER134 upon binding to 3-oxo-6-HSL. Additionally, alkyl and pi-alkyl interactions are observed with residues TYR63, TYR71, PHE59, VAL68, LEU106, PHE100, ALA110, and VAL82. In contrast, the modeled SdiA of *K. pneumoniae*, which was built using the *E. coli* SdiA structure (PDB ID: 4Y15) as a template, exhibits a docking score of -7.626 kcal/mol with 3-oxo-6-HSL using Auto dock Vina. The ligand binding in the *K. pneumoniae* SdiA model results in hydrogen bonds with TRP67, TYR63, ASP80, CYS45, and SER134, while alkyl and pi-alkyl interactions are observed with PHE77, TYR71, PHE59, VAL82, PHE100, LEU106, and TRP95. Importantly, the ligand binds to the same active site in both proteins with the same orientation, indicating that the docking site in the modeled protein is appropriate. The pose of the ligand in both proteins is identical, further supporting the validity of the modeled protein and its predicted active site for docking studies. In conclusion, Figure 2 provides a comparative analysis of the interactions between 3-oxo-6-HSL and SdiA proteins from *E. coli* and *K. pneumoniae*. Despite some differences in the interacting residues, the overall binding mode and orientation of the ligand are conserved in both species. This suggests that the modeled *K. pneumoniae* SdiA protein could be a suitable target for further docking studies aimed at understanding the role of quorum sensing in this organism.

#### **Docking of modelled SdiA with different AI-1 and AI-2 signals as ligands**

Molecular docking is a computational approach that predicts how a ligand will bind to a protein or nucleic acid, such as a receptor or enzyme, by determining the most favorable orientation. This technique provides valuable insights into the binding mode, affinity, and interactions between the ligand and the protein. AutoDock Vina is a widely used open-source software that enables accurate and rapid prediction of protein-ligand complexes. In this study, AutoDock Vina was employed to explore the binding of various AI-1 and AI-2 to the modelled SdiA protein of *Klebsiella pneumoniae*. Table 2 shows the docking energies of each AI-1 and AI-2 with their respective ranks based on the AutoDock Vina scores.

The primary aim of this investigation was to identify the top-ranking ligands based on docking scores and gain a better understanding of their interactions with the protein. Additionally, the two worst ligands in terms of docking energy were also discussed. The interactions made by the top four ligands are illustrated in 2D in Figure 3 and 3D in Figure 4.

The docking energies are reported in kcal/mol, and the lower the energy, the higher the binding affinity of the ligand to the protein receptor. The top 4 ligands based on their docking scores are 3-OH-C10-HSL, 3-OH-C8-HSL, 3-oxo-C10-HSL, and 3-oxo-C8-HSL. These four ligands show the highest binding affinity to the SdiA protein with docking energies of -8.907, -8.887, -8.807, and -8.759 kcal/mol, respectively.

The interaction types between these four ligands and the amino acids of SdiA are also provided in Table 2. These interactions include hydrogen bonds, carbon-hydrogen bonds, pi-sigma bonds, and pi-pi/pi-alkyl bonds. These interactions are important for the stabilization of the ligand-receptor complex, and they contribute to the binding affinity of the ligand to the protein receptor.

For instance, the top-ranking ligand, 3-OH-C10-HSL, interacts with four amino acids in the protein receptor, including TYR63, TRP67, ASP80, and SER134, through hydrogen bonds. In addition, it forms carbon-hydrogen bonds with nine other amino acids, including CYS45, PHE59, TYR71, PHE77, VAL82, TRP95, PHE100, LEU106, and ALA110. The other three top-scoring ligands also interact with a similar set of amino acids, albeit with slightly different interaction types and patterns.

Other ligands, such as C10-HSL, 3-oxo-C12-HSL, 3-OH-C6-HSL, C6-HSL, 3-oxo-C6-HSL, C8-HSL, and C4-HSL, show relatively lower binding affinity to the SdiA protein, with docking energies ranging from -7.583 to -6.042 kcal/mol. These ligands interact with fewer amino acids in the protein receptor and with fewer interaction types. For instance, C4-HSL interacts only with two amino acids, TYR63 and TRP67, through pi-pi/pi-alkyl bonds. C8-HSL interacts with nine amino acids through carbon-hydrogen bonds and pi-pi/pi-alkyl bonds.

Furthermore, the worst two ligands in terms of binding affinity are THMF and HMF, with docking energies of -4.360 and -3.768 kcal/mol, respectively. These ligands interact with only a few amino acids in the protein receptor, and their interaction types are limited to pi-pi/pi-alkyl bonds.

In the present study, we utilized AutoDock Vina to conduct molecular docking of Acyl-Homoserine Lactones (AHLs) with the modelled SdiA protein of *Klebsiella pneumoniae*. The docking results revealed 3-OH-C10-HSL, 3-OH-C8-HSL, 3-oxo-C10-HSL, and 3-oxo-C8-HSL as the top four ligands, exhibiting high binding affinities and forming crucial hydrogen bonds with key amino acids of SdiA. Conversely, THMF and HMF showed lower docking energies and fewer interactions, making them the two worst ligands. These findings offer valuable insights into the binding mechanisms of AHLs with SdiA, which can guide the development of innovative therapeutic approaches for regulating quorum sensing in *K. pneumoniae*.

Molecular docking with AutoDock Vina was then used to investigate the specific interactions and ligand preferences of SdiA with various AHLs and AI-2. Molecular docking is a computational approach that predicts how a ligand will bind to a protein or nucleic acid, such as a receptor or enzyme, by determining the most favorable orientation [31]. AutoDock Vina is a widely used open-source software that enables accurate and rapid prediction of protein-ligand complexes [23]. The present study utilized AutoDock Vina [32] to dock various AHLs and AI-2 ligands with the modelled SdiA protein of *K. pneumoniae*. These findings offer valuable insights into the binding mechanisms of AHLs with SdiA, which can guide the development of innovative therapeutic approaches for regulating quorum sensing in *K. pneumoniae*.

Several previous studies have also investigated the role of SdiA in *K. pneumoniae* and its interaction with various AHLs [28]. For instance, a study by Zheng and colleagues in the year 2018 identified that SdiA is required for the expression of several virulence factors in *K. pneumoniae*, and its activity is regulated by AHLs produced by other bacterial species [33]. Another study by Ahmed M. Z. and colleagues in the year 2021 showed that SdiA can bind to a range of AHLs, including 3-oxo-C12-HSL, 3-oxo-C10-HSL, and C10-HSL, and that this binding is crucial for the expression of fimbriae and capsule polysaccharide biosynthesis in *K. pneumoniae* [26]. Furthermore, a study by Zhang and colleagues in the year 2019 investigated the role of SdiA in regulating the expression of type III secretion system in *K. pneumoniae* and found that this regulation is mediated by AHLs produced by other bacterial species.

AHL receptors are known to exhibit degeneracy, as they can interact with multiple AHL signals, allowing bacteria to eavesdrop on the quorum sensing signals of other bacterial species in mixed microbial communities [6]. This phenomenon has been observed in various AHL receptor systems, such as LuxR in *Vibrio fischeri* and LasR in *Pseudomonas aeruginosa* [34]. The degeneracy of AHL receptors suggests that they may have evolved to respond to a range of different AHL signals, allowing bacteria to adapt to changing environments and communicate with a diverse range of microbial species.

Quantifying the conformational flexibility of proteins with and without ligands and inhibitors is crucial for understanding protein function and regulatory mechanisms. AHL transcriptional regulators, which undergo conformational changes upon binding to AHL signals, can serve as a model system to explore the implications of conformational change on gene expression [7]. Additionally, the structural analysis of AHL-QS systems may provide insights into the development of site-specific or allosteric inhibitors that can selectively target bacterial virulence without affecting bacterial viability.

Further research is necessary to understand how the AHL-QS system interacts with host cells and to develop novel anti-virulence approaches as a potential future antimicrobial strategy. The AHL-QS system can also help researchers better understand the fundamental regulatory framework for gene expression in prokaryotes. Overall, understanding the diversity and complexity of the AHL-QS system is essential for developing effective strategies to combat bacterial infections.

The present study contributes to the existing literature on the role of SdiA in *K. pneumoniae* and its interaction with various AHLs, providing valuable insights into the ligand preferences and interactions of SdiA with AHLs and AI-2. These findings have implications for the development of innovative therapeutic

approaches for regulating quorum sensing in *K. pneumoniae*. However, further studies are necessary to validate these findings and develop effective inhibitors for SdiA. The study utilized homology modelling [28] and molecular docking to investigate the behavior of SdiA with AHLs and AI-2, highlighting the importance of computational approaches in understanding the molecular mechanisms underlying bacterial quorum sensing.

In conclusion, the results of our molecular docking study provide insights into the degeneracy of SdiA in *Klebsiella pneumoniae* and shed light on its ability to bind to various AHLs and AI-2 ligands. The study reveals that SdiA shows a high degree of promiscuity in ligand binding, allowing it to interact with multiple AHLs and potentially AI-2, providing functional advantages to *K. pneumoniae* in mixed microbial communities. The identified ligands, 3-OH-C10-HSL, 3-OH-C8-HSL, 3-oxo-C10-HSL, and 3-oxo-C8-HSL, exhibit strong binding affinities with SdiA and form crucial hydrogen bonds with key amino acids, while THMF and HMF show poor docking scores. These findings offer a basis for developing novel therapeutic strategies to modulate quorum sensing in *K. pneumoniae*, which is crucial in controlling the expression of virulence factors and can potentially guide the development of innovative approaches to combat *K. pneumoniae* infections. Therefore, our study provides valuable insights into the degeneracy of SdiA in *K. pneumoniae*, which can be used to develop new strategies for combating antibiotic resistance in this pathogen.

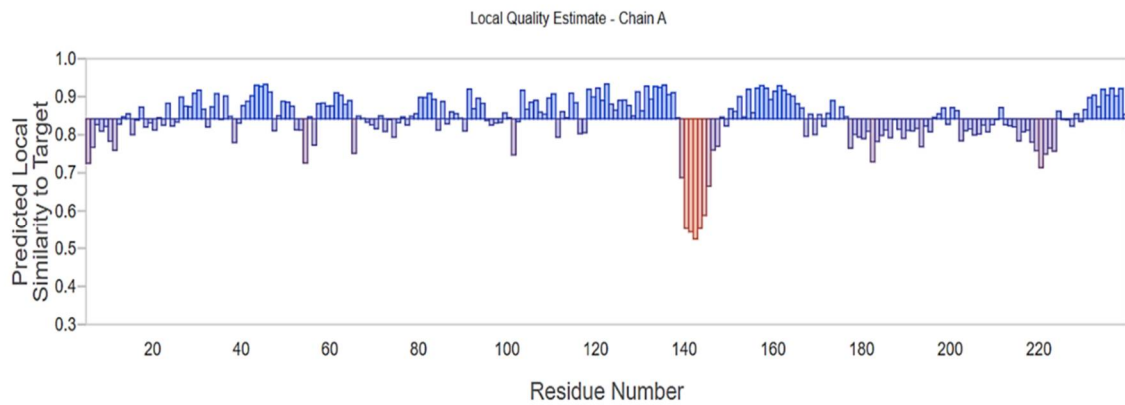
**Table 1 Various AHLs produced by Gram negative bacteria.**

AI-1/AI-2	Producing bacteria	References
<b>3-oxo-C6-HSL</b>	<i>Vibrio fischeri</i> , <i>Pseudomonas aeruginosa</i> , <i>Aeromonas hydrophila</i> , <i>Burkholderia cepacia</i> , <i>Burkholderia pseudomallei</i>	[35], [36], [37]
<b>3-oxo-C8-HSL</b>	<i>Agrobacterium tumefaciens</i> , <i>Burkholderia cepacia</i> , <i>Burkholderia pseudomallei</i>	[38], [39]
<b>3-oxo-C10-HSL</b>	<i>Burkholderia cepacia</i> , <i>Burkholderia pseudomallei</i>	[39], [40]
<b>3-oxo-C12-HSL</b>	<i>Burkholderia cepacia</i> , <i>Burkholderia pseudomallei</i>	[41], [42]
<b>3-OH-C6-HSL</b>	<i>Pseudomonas aeruginosa</i> , <i>Aeromonas hydrophila</i>	[39], [43]
<b>3-OH-C8-HSL</b>	<i>Pseudomonas aeruginosa</i>	[44]
<b>3-OH-C10-HSL</b>	<i>Pseudomonas aeruginosa</i>	[45]
<b>C4-HSL</b>	<i>Vibrio fischeri</i> , <i>Agrobacterium tumefaciens</i> , <i>Yersinia enterocolitica</i> , <i>Erwinia carotovora</i> , <i>Escherichia coli</i> , <i>Chromobacterium violaceum</i>	[35], [46], [47]
<b>C6-HSL</b>	<i>Yersinia enterocolitica</i> , <i>Erwinia carotovora</i> , <i>Escherichia coli</i> , <i>Chromobacterium violaceum</i>	[46], [48]
<b>C8-HSL</b>	<i>Erwinia carotovora</i> , <i>Serratia liquefaciens</i> , <i>Escherichia coli</i> , <i>Chromobacterium violaceum</i>	[49], [50]
<b>C10-HSL</b>	<i>Serratia liquefaciens</i> , <i>Escherichia coli</i> , <i>Chromobacterium violaceum</i>	[51]
<b>THMF</b>	<i>Vibrio harveyi</i> , <i>Vibrio cholerae</i> , <i>Vibrio parahaemolyticus</i> , <i>Vibrio vulnificus</i> , <i>Vibrio anguillarum</i>	[52]
<b>HMF</b>	<i>Salmonella typhimurium</i> , <i>Escherichia coli</i> , <i>Agrobacterium tumefaciens</i> , <i>Sinorhizobium meliloti</i> , <i>Erwinia carotovora</i>	[38]

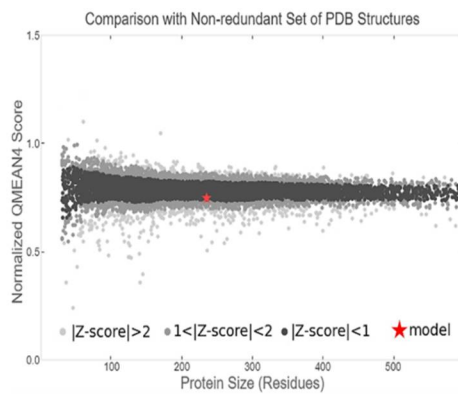
**Table 2 Docking energies of AHLs predicted for its binding with modelled SdiA of *Klebsiella pneumoniae*.**

AI-1/AI-2	Docking energy (kcal/mol)	Ranks	Interaction types with amino-acids of SdiA			
			H-bonds	Carbon-Hydrogen bond	Pi-Sigma	Pi-Pi/Pi-Alkyl bonds
3-OH-C10-HSL	-8.907	1	TYR63, TRP67, ASP80, SER134			CYS45, PHE59, TYR71, PHE77, VAL82, TRP95, PHE100, LEU106, ALA110
3-OH-C8-HSL	-8.887	2	TYR63, TRP67, ASP80, SER134			PHE59, TYR71, VAL82, PHE100, LEU106, ALA110
3-oxo-C10-HSL	-8.807	3	TYR63, TRP67, ASP80	THR43, SER134	TYR71	PHE59, MET68, VAL82, TRP95, PHE100, LEU106, ALA110
3-oxo-C8-HSL	-8.759	4	CYS45, TYR63, TRP67, ASP80, SER134			PHE59, MET68, TYR71, VAL71, TRP95, PHE100, LEU106
3-oxo-C12-HSL	-7.756	5	TYR63, TRP67, ASP80, SER134	TYR63, TRP67, ASP80, SER134		CYS45, PHE59, MET68, TYR71, PHE77, VAL82, LEU83, TRP95, PHE100, LEU106, ALA110
3-OH-C6-HSL	-7.626	6	TYR63, TRP67, ASP80, SER134			PHE59, TYR71, PHE77, VAL82, TRP95, PHE100, ALA110
C10-HSL	-7.583	7	TYR63, TRP67, ASP80	SER134		CYS45, PHE59, MET68, TYR71, PHE77, VAL82, LEU83, TRP95, PHE100, LEU106
C6-HSL	-7.053	8	TYR63, TRP67, ASP80		TYR71	PHE59, PHE77, VAL82, TRP95, PHE100, LEU106,
3-oxo-C6-HSL	-7.026	9	CYS45, TYR63, TRP67, ASP80, SER134			PHE59, TYR71, PHE77, VAL82, TRP95, PHE100, LEU106
C8-HSL	-6.66	10	TYR63, TRP67, ASP80, SER134			CYS45, PHE59, MET68, TYR71, PHE77, VAL82, TRP95, PHE100, LEU106
C4-HSL	-6.042	11	TYR63, TRP67, ASP80, SER134			VAL82, TRP95, PHE100, LEU106,
THMF	-4.360	12	TYR63, ASP80, SER134			TYR71, VAL82
HMF	-3.768	13	TYR63, TRP67			TRP95, PHE100, LEU106, ALA110

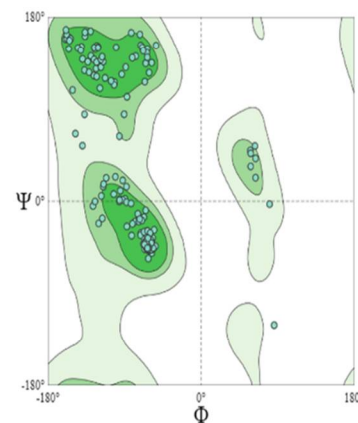
(a) QMEANDisCo Global: **0.84**  $\pm$  0.05



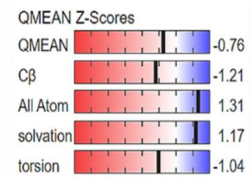
(b)



(c)



(d)



(e)

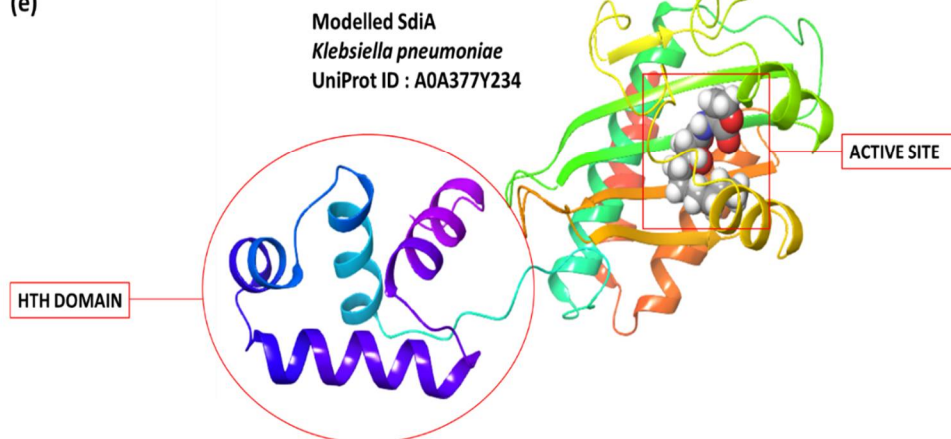


**Figure 1** Quality check of modelled SdiA of *Klebsiella pneumoniae* using template 4Y15 (PDB) where (a) represents Local Quality estimate (b) Normalized QMEAN score, (c) Ramachandran plot, (d) QMEAN Z-SCORES (e) Structure of modelled SdiA, its active site and HTH domain.

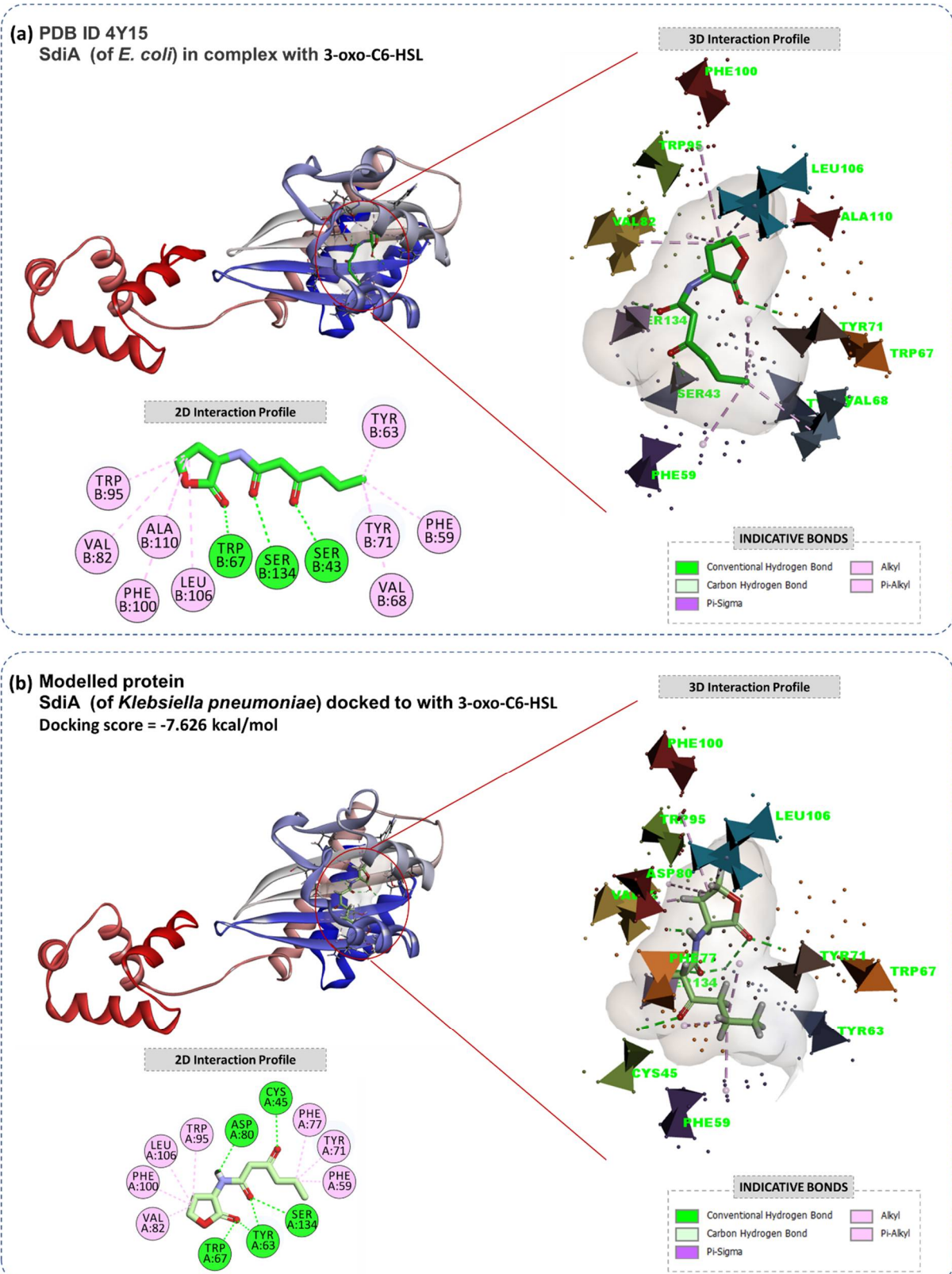
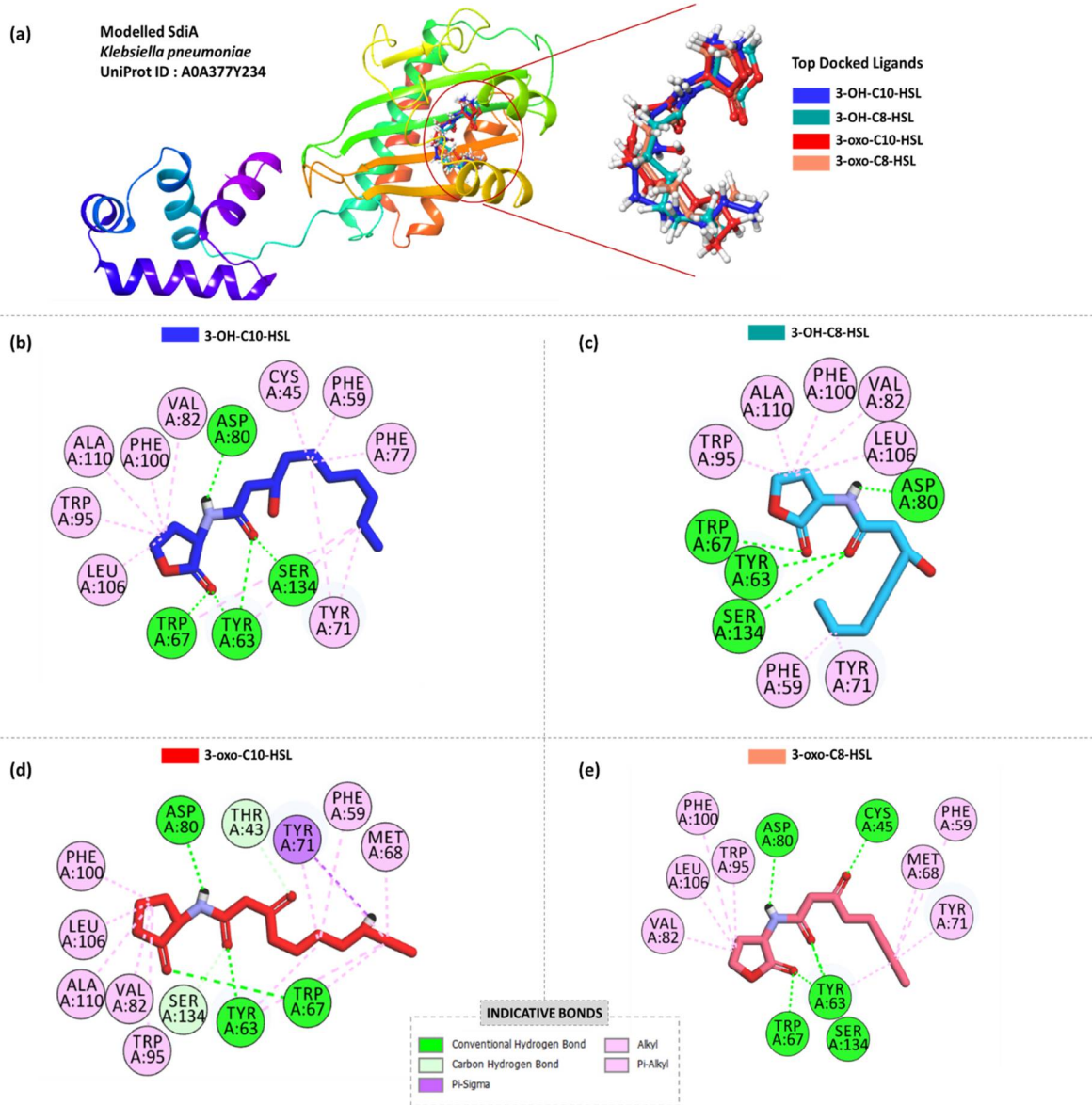
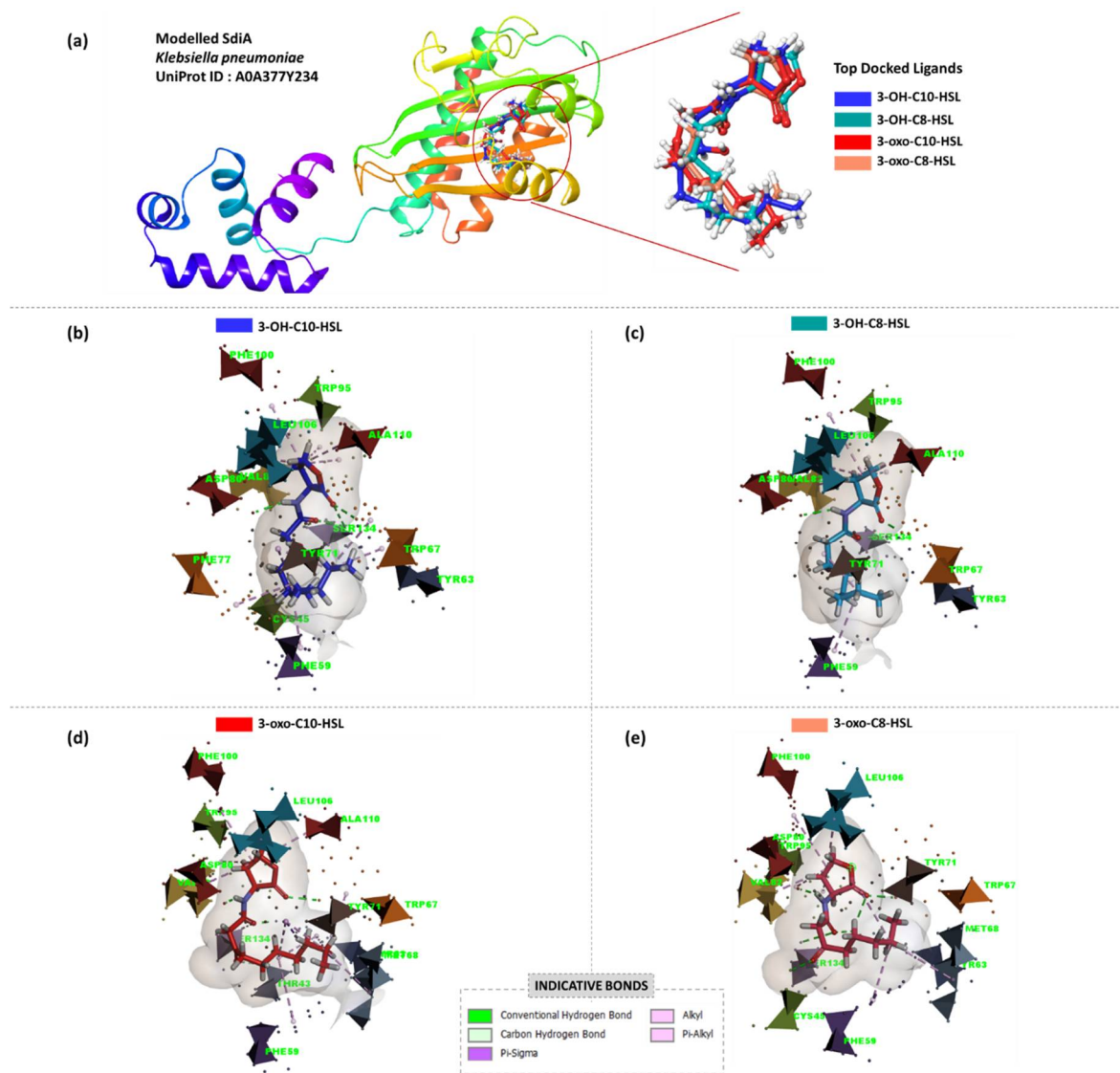


Figure 2 Assessing the interaction of 3-oxo-C6-HSL with (a) SdiA of *E. coli* PDB ID 4Y15, (b) SdiA of *K. pneumoniae*.



**Figure 3 Docking of various AHLs with modelled SdiA, where 2D interaction of amino acids with (a) 3-OH-C10-HSL, (b) 3-OH-C8-HSL, (c) 3-oxo-C10-HSL and (d) 3-oxo-C8-HSL is shown**



**Figure 4 Docking of various AHLs with modelled SdiA, where 2D interaction of amino acids with (a) 3-OH-C10-HSL, (b) 3-OH-C8-HSL, (c) 3-oxo-C10-HSL and (d) 3-oxo-C8-HSL is shown.**

## ACKNOWLEDGEMENTS

Authors acknowledge DST-FIST Sponsored Department of Microbiology and Biotechnology, School of Sciences, Gujarat University, for providing necessary facilities to perform experiments and GSBTM (DST, Government of Gujarat) for providing Bioinformatics Node facility.

## FUNDING

This work was supported by Gujarat State Biotechnology Mission (GSBTM) under Network program on Antimicrobial Resistance, Superbugs, and One Health: Human Health Care Node [GSBTM/JD(R&D)/616/21-22/1236]

## REFERENCES

1. R. Podschun and U. Ullmann, "Klebsiella spp. as nosocomial pathogens: Epidemiology, taxonomy, typing methods, and pathogenicity factors," *Clin. Microbiol. Rev.*, vol. 11, no. 4, pp. 589–603, 1998, doi: 10.1128/cmr.11.4.589.
2. R. M. Martin and M. A. Bachman, "Colonization, infection, and the accessory genome of *Klebsiella pneumoniae*," *Front. Cell. Infect. Microbiol.*, vol. 8, no. JAN, 2018, doi: 10.3389/fcimb.2018.00004.
3. S. Indrajith *et al.*, "Molecular insights of Carbapenem resistance *Klebsiella pneumoniae* isolates with focus on multidrug resistance from clinical samples," *J. Infect. Public Health*, vol. 14, no. 1, pp. 131–138, 2021, doi: 10.1016/j.jiph.2020.09.018.
4. S. B. Tay and W. S. Yew, "Development of quorum-based anti-virulence therapeutics targeting Gram-negative

- bacterial pathogens,” *Int. J. Mol. Sci.*, vol. 14, no. 8, pp. 16570–16599, 2013, doi: 10.3390/ijms140816570.
5. T. R. De Kievit and B. H. Iglewski, “Bacterial quorum sensing in pathogenic relationships,” *Infect. Immun.*, vol. 68, no. 9, pp. 4839–4849, 2000, doi: 10.1128/IAI.68.9.4839-4849.2000.
  6. M. Schuster, D. Joseph Sexton, S. P. Diggle, and E. Peter Greenberg, “Acyl-homoserine lactone quorum sensing: From evolution to application,” *Annu. Rev. Microbiol.*, vol. 67, pp. 43–63, 2013, doi: 10.1146/annurev-micro-092412-155635.
  7. R. Czajkowski and S. Jafra, “Quenching of acyl-homoserine lactone-dependent quorum sensing by enzymatic disruption of signal molecules,” *Acta Biochim. Pol.*, vol. 56, no. 1, pp. 1–16, 2009, doi: 10.18388/abp.2009\_2512.
  8. M. E. A. Churchill and L. Chen, “Structural basis of acyl-homoserine lactone-dependent signaling,” *Chem. Rev.*, vol. 111, no. 1, pp. 68–85, 2011, doi: 10.1021/cr1000817.
  9. W. R. J. D. Galloway, J. T. Hodgkinson, S. D. Bowden, M. Welch, and D. R. Spring, “Quorum sensing in Gram-negative bacteria: Small-molecule modulation of AHL and AI-2 quorum sensing pathways,” *Chem. Rev.*, vol. 111, no. 1, pp. 28–67, 2011, doi: 10.1021/cr100109t.
  10. R. Daniels, J. Vanderleyden, and J. Michiels, “Quorum sensing and swarming migration in bacteria,” *FEMS Microbiol. Rev.*, vol. 28, no. 3, pp. 261–289, 2004, doi: 10.1016/j.femsre.2003.09.004.
  11. B. Li, Y. Zhao, C. Liu, Z. Chen, and D. Zhou, “Molecular pathogenesis of *Klebsiella pneumoniae*,” *Future Microbiol.*, vol. 9, no. 9, pp. 1071–1081, 2014, doi: 10.2217/fmb.14.48.
  12. T. Pacheco *et al.*, “SdiA, a Quorum-Sensing Regulator, Suppresses Fimbriae Expression, Biofilm Formation, and Quorum-Sensing Signaling Molecules Production in *Klebsiella pneumoniae*,” *Front. Microbiol.*, vol. 12, 2021, doi: 10.3389/fmicb.2021.597735.
  13. J. Vornhagen *et al.*, “A plasmid locus associated with *Klebsiella* clinical infections encodes a microbiomedependent gut fitness factor,” *PLoS Pathog.*, vol. 17, no. 4, 2021, doi: 10.1371/journal.ppat.1009537.
  14. O. Rendueles and J. M. Ghigo, “Mechanisms of competition in biofilm communities,” *Microb. Biofilms*, pp. 319–342, 2015, doi: 10.1128/9781555817466.ch16.
  15. R. P. Ryan and J. M. Dow, “Diffusible signals and interspecies communication in bacteria,” *Microbiology*, vol. 154, no. 7, pp. 1845–1858, 2008, doi: 10.1099/mic.0.2008/017871-0.
  16. M. J. Federle, “Autoinducer-2-based chemical communication in bacteria: Complexities of interspecies signaling,” *Contrib. Microbiol.*, vol. 16, pp. 18–32, 2009, doi: 10.1159/000219371.
  17. N. Guex, M. C. Peitsch, and T. Schwede, “Automated comparative protein structure modeling with SWISS-MODEL and Swiss-PdbViewer: A historical perspective,” *Electrophoresis*, vol. 30, no. SUPPL. 1, 2009, doi: 10.1002/elps.200900140.
  18. P. Benkert, M. Biasini, and T. Schwede, “Toward the estimation of the absolute quality of individual protein structure models,” *Bioinformatics*, vol. 27, no. 3, pp. 343–350, 2011, doi: 10.1093/bioinformatics/btq662.
  19. C. Colovos and T. O. Yeates, “Verification of protein structures: Patterns of nonbonded atomic interactions,” *Protein Sci.*, vol. 2, no. 9, pp. 1511–1519, 1993, doi: 10.1002/pro.5560020916.
  20. S. Müller, T. Löhne, and A. V. Krivov, “The debris disk of Vega: A steady-state collisional cascade, naturally,” *Astrophys. J.*, vol. 708, no. 2, pp. 1728–1747, 2010, doi: 10.1088/0004-637X/708/2/1728.
  21. G. G. Krivov, M. V. Shapovalov, and R. L. Dunbrack, “Improved prediction of protein side-chain conformations with SCWRL4,” *Proteins Struct. Funct. Bioinforma.*, vol. 77, no. 4, pp. 778–795, 2009, doi: 10.1002/prot.22488.
  22. A. W. Sousa Da Silva and W. F. Vranken, “ACPYPE - AnteChamber PYthon Parser interfacE,” *BMC Res. Notes*, vol. 5, pp. 1–8, 2012, doi: 10.1186/1756-0500-5-367.
  23. J. Gasteiger and C. Jochum, “An algorithm for the perception of synthetically important rings,” *J. Chem. Inf.*, vol. 19, no. 1, pp. 43–48, 1979.
  24. O. Trott and A. J. Olson, “AutoDock Vina: Improving the speed and accuracy of docking with a new scoring function, efficient optimization, and multithreading,” *J. Comput. Chem.*, p. NA-NA, 2009, doi: 10.1002/jcc.21334.
  25. P. Rao *et al.*, “Reckoning a fungal metabolite, Pyranonigrin A as a potential Main protease (Mpro) inhibitor of novel SARS-CoV-2 virus identified using docking and molecular dynamics simulation,” *Biophys. Chem.*, p. 106425, Jul. 2020, doi: 10.1016/j.bpc.2020.106425.
  26. M. Z. Ahmed *et al.*, “Identifying novel inhibitor of quorum sensing transcriptional regulator (SdiA) of *Klebsiella pneumoniae* through modelling, docking and molecular dynamics simulation,” *J. Biomol. Struct. Dyn.*, vol. 39, no. 10, pp. 3594–3604, 2021, doi: 10.1080/07391102.2020.1767209.
  27. L. Steindler and V. Venturi, “Detection of quorum-sensing N-acyl homoserine lactone signal molecules by bacterial biosensors,” *FEMS Microbiol. Lett.*, vol. 266, no. 1, pp. 1–9, 2007, doi: 10.1111/j.1574-6968.2006.00501.x.
  28. A. Hillisch, L. F. Pineda, and R. Hilgenfeld, “Utility of homology models in the drug discovery process,” *Drug Discov. Today*, vol. 9, no. 15, pp. 659–669, 2004, doi: 10.1016/S1359-6446(04)03196-4.
  29. J. Li *et al.*, “Structure and function analysis of nucleocapsid protein of tomato spotted wilt virus interacting with RNA using homology modeling,” *J. Biol. Chem.*, vol. 290, no. 7, pp. 3950–3961, 2015, doi: 10.1074/jbc.M114.604678.
  30. S. R. Villa *et al.*, “Homology modeling of FFA2 identifies novel agonists that potentiate insulin secretion,” *J. Invest. Med.*, vol. 65, no. 8, pp. 1116–1124, 2017, doi: 10.1136/jim-2017-000523.
  31. G. Sliwoski, S. Kothiwale, J. Meiler, and E. W. Lowe, “Computational methods in drug discovery,” *Pharmacol. Rev.*, vol. 66, no. 1, pp. 334–395, 2014, doi: 10.1124/pr.112.007336.
  32. C. Barbey *et al.*, “A rhodococcal transcriptional regulatory mechanism detects the common lactone ring of AHL quorum-sensing signals and triggers the quorum-quenching response,” *Front. Microbiol.*, vol. 9, no. NOV, 2018, doi: 10.3389/fmicb.2018.02800.

33. J. X. Zheng *et al.*, "Biofilm formation in *Klebsiella pneumoniae* bacteremia strains was found to be associated with CC23 and the presence of *wcaG*," *Front. Cell. Infect. Microbiol.*, vol. 8, no. FEB, 2018, doi: 10.3389/fcimb.2018.00021.
34. P. Parmar, A. Shukla, P. Rao, M. Saraf, B. Patel, and D. Goswami, "The rise of gingerol as anti-QS molecule: Darkest episode in the LuxR-mediated bioluminescence saga," *Bioorg. Chem.*, vol. 99, p. 103823, 2020, doi: 10.1016/j.bioorg.2020.103823.
35. S. Atkinson and P. Williams, "Quorum sensing and social networking in the microbial world," *J. R. Soc. Interface*, vol. 6, no. 40, pp. 959–978, 2009, doi: 10.1098/rsif.2009.0203.
36. K. Y. How, K. W. Hong, and K. G. Chan, "Whole genome sequencing enables the characterization of *BurI*, a LuxI homologue of *Burkholderia cepacia* strain GG4," *PeerJ*, vol. 2015, no. 8, 2015, doi: 10.7717/peerj.1117.
37. Y. Tashiro, Y. Yawata, M. Toyofuku, H. Uchiyama, and N. Nomura, "Interspecies interaction between *Pseudomonas aeruginosa* and other microorganisms," *Microbes Environ.*, vol. 28, no. 1, pp. 13–24, 2013, doi: 10.1264/jisme.2013.01.0167.
38. P. Lumijaktase *et al.*, "Quorum sensing regulates *dpsA* and the oxidative stress response in *Burkholderia pseudomallei*," *Microbiology*, vol. 152, no. 12, pp. 3651–3659, 2006, doi: 10.1099/mic.0.29226-0.
39. J. Zhu, J. W. Beaber, M. I. Moré, C. Fuqua, A. Eberhard, and S. C. Winans, "Analogues of the autoinducer 3-oxooctanoyl-homoserine lactone strongly inhibit activity of the TraR protein of *Agrobacterium tumefaciens*," *J. Bacteriol.*, vol. 180, no. 20, pp. 5398–5405, 1998, doi: 10.1128/jb.180.20.5398-5405.1998.
40. L. Eberl and K. Riedel, "Mining quorum sensing regulated proteins - Role of bacterial cell-to-cell communication in global gene regulation as assessed by proteomics," *Proteomics*, vol. 11, no. 15, pp. 3070–3085, 2011, doi: 10.1002/pmic.201000814.
41. S. P. Diggle *et al.*, "Functional Genetic Analysis Reveals a 2-Alkyl-4-Quinolone Signaling System in the Human Pathogen *Burkholderia pseudomallei* and Related Bacteria," *Chem. Biol.*, vol. 13, no. 7, pp. 701–710, 2006, doi: 10.1016/j.chembiol.2006.05.006.
42. K. Riedel *et al.*, "Computer-aided design of agents that inhibit the *cep* quorum-sensing system of *Burkholderia cenocepacia*," *Antimicrob. Agents Chemother.*, vol. 50, no. 1, pp. 318–323, 2006, doi: 10.1128/AAC.50.1.318-323.2006.
43. Z. Yu *et al.*, "Identification and characterization of a LuxI/R-type quorum sensing system in *Pseudoalteromonas*," *Res. Microbiol.*, vol. 170, no. 6–7, pp. 243–255, 2019, doi: 10.1016/j.resmic.2019.07.001.
44. S. Li, S. Wu, Y. Ren, Q. Meng, J. Yin, and Z. Yu, "Characterization of differentiated autoregulation of LuxI/LuxR-type quorum sensing system in *Pseudoalteromonas*," *Biochem. Biophys. Res. Commun.*, vol. 590, pp. 177–183, 2022, doi: 10.1016/j.bbrc.2021.12.107.
45. M. Mattiuzzo *et al.*, "The plant pathogen *Pseudomonas fuscovaginae* contains two conserved quorum sensing systems involved in virulence and negatively regulated by RsaL and the novel regulator RsaM," *Environ. Microbiol.*, vol. 13, no. 1, pp. 145–162, 2011, doi: 10.1111/j.1462-2920.2010.02316.x.
46. K. Winzer, C. Falconer, N. C. Garber, S. P. Diggle, M. Camara, and P. Williams, "The *Pseudomonas aeruginosa* lectins PA-IL and PA-IIL are controlled by quorum sensing and by RpoS," *J. Bacteriol.*, vol. 182, no. 22, pp. 6401–6411, 2000, doi: 10.1128/JB.182.22.6401-6411.2000.
47. E. A. Yates *et al.*, "N-acylhomoserine lactones undergo lactonolysis in a pH-, temperature-, and acyl chain length-dependent manner during growth of *Yersinia pseudotuberculosis* and *Pseudomonas aeruginosa*," *Infect. Immun.*, vol. 70, no. 10, pp. 5635–5646, 2002, doi: 10.1128/IAI.70.10.5635-5646.2002.
48. S. Atkinson, C. Y. Chang, R. E. Sockett, M. Cámara, and P. Williams, "Quorum sensing in *Yersinia enterocolitica* controls swimming and swarming motility," *J. Bacteriol.*, vol. 188, no. 4, pp. 1451–1461, 2006, doi: 10.1128/JB.188.4.1451-1461.2006.
49. B. Smadja, X. Latour, D. Faure, S. Chevalier, Y. Dessaux, and N. Orange, "Involvement of N-acylhomoserine lactones throughout plant infection by *Erwinia carotovora* subsp. *atroseptica* (*Pectobacterium atrosepticum*)," *Mol. Plant-Microbe Interact.*, vol. 17, no. 11, pp. 1269–1278, 2004, doi: 10.1094/MPMI.2004.17.11.1269.
50. M. T. G. Holden *et al.*, "Quorum-sensing cross talk: Isolation and chemical characterization of cyclic dipeptides from *Pseudomonas aeruginosa* and other Gram-negative bacteria," *Mol. Microbiol.*, vol. 33, no. 6, pp. 1254–1266, 1999, doi: 10.1046/j.1365-2958.1999.01577.x.
51. B. Hidalgo-Romano *et al.*, "Indole inhibition of N-acylated homoserine lactone-mediated quorum signalling is widespread in Gram-negative bacteria," *Microbiol. (United Kingdom)*, vol. 160, pp. 2464–2473, 2014, doi: 10.1099/mic.0.081729-0.
52. C. A. Lowery, T. J. Dickerson, and K. D. Janda, "Interspecies and interkingdom communication mediated by bacterial quorum sensing," *Chem. Soc. Rev.*, vol. 37, no. 7, pp. 1337–1346, 2008, doi: 10.1039/b702781h.

**Copyright: © 2023 Author.** This is an open access article distributed under the Creative Commons Attribution License, which permits unrestricted use, distribution, and reproduction in any medium, provided the original work is properly cited.